Detection of moving targets in SAR

A.N. Leukhin[1] V.I. Bezrodny[1], A.A. Voronin[1], N.V. Kokovihina[1]
[1]Mari State University, Lenin Sq. 1, Yoshkar-Ola, Russia, 424000

Abstract. Radar with ground moving target indication (GMTI) is intended to isolate the signals of moving targets from the whole mass of signals reflected by different objects. In this work, we investigate two approaches to form GMIT images: displaced phase center antenna algorithm (DPCA) and along-track interferometry algorithm (ATI) by using the mathematical model of SAR.

Keywords: Detection of moving targets, low level sidelobes, synthetic aperture radar.

1. Introduction

The moving target indication (MTI) in radars was realized at the end of the Second World War on the basis of acoustic delay lines and became widely used in the postwar period. However, a direct indication made it possible to distinguish only very bright objects, such as airplanes and ships. Later, the systems began to use phase detectors, which significantly reduced the effect of noise. In the 70's and 80's, systems were spread that, by filtering in several speed channels, were able to determine the speed of movement. Modern moving target indication systems are divided into various types such as airborne MTI (AMTI), ground MTI (GMTI) or combined stationary and moving target indication (SMTI).

In parallel to the development of MTI, in the 50 years of the 20th century, the technology of synthetic aperture radar (SAR) was invented. Visualization using radars with synthetic aperture is a technique that allows to significantly increase the resolving power of a radar in the direction transverse with respect to the direction of flight and to obtain a detailed image of the radar map of the terrain above which the flight of the aircraft.

Imaging features in radars with a synthesized aperture with the transition to a two-dimensional plane allow using different approaches for the implementation of GMTI. In this paper, we compare two algorithms: displaced phase center antenna (DPCA) and along-track interferometry (ATI) utilizing methods of mathematical modeling.

2. The implementation details of the mathematical model

In the process of modeling a radar image, the problem of constructing electrodynamic and statistical models of the scene.

In our work, we use a combined approach to get a scattered field. Small metal objects (like cars) on the scene are processed by a combination of approximate methods: Physical Optics (PO) + Physical Theory of Diffraction (PTD). These methods are described in works [1–5]. The most interesting papers [1–3] describe the calculations of scattered fields, give complete formulas and taking into account polarization effects.

From the other side, approximate methods mentioned above are not fit for dielectric materials and large-scale objects. So, all underlying surface processed with a statistical approach. We

have prepared 11 types of materials with respect to polarisation and slipping angle, data was collected from works [6–8].

To model the reflection of the signal from the surface, we used a model of a polygonal surface, representing a surface in the form of a set of elementary elements finite sizes. In this case, the facet size should be less than the resolving power of radar.

Thus, the total scattered field on the stage is calculated as follows, as represented in equation 1.

$$\vec{E}_{scatt} = \vec{E}_1 + \vec{E}_2 + \vec{E}_3 + \vec{E}_4, \tag{1}$$

where $\vec{E}_1$ — the vector of the field strength corresponding to the field scattered on the smooth parts of the scene, $\vec{E}_1$ — the field strength vector corresponding to scattering on sharp edges, $\vec{E}_3$ — field strength vector arising at multiple reflections, $\vec{E}_4$ — the field intensity vector is scattered from the underlying surface.

3. Displaced phase center antenna algorithm

Displaced phase center antenna or (DPCA) implements the usual way to achieve SAR GMTI data as it implements in radar MTI. Two antennas mounted along flight direction, both of them are used to create independent complex radar images. The key operation in DPCA is subtraction one complex image from another as shown in figure 1. The idea is that the same patch ground is on the same pixel on the two images, and the response difference is effectively compensated between the two channels in amplitude and phase.

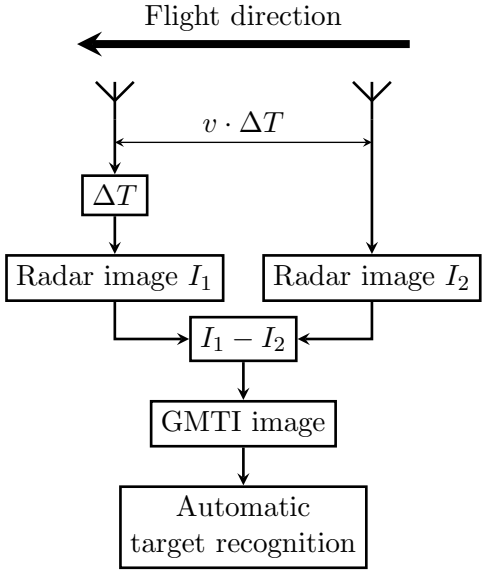

Figure 1. Image processing scheme using the DPCA algorithm.

The system should delay the first image by the amount of time corresponding to the distance between pulses; in that ratio flight speed v is used.

Figure 2 shows point distribution in DPCA GMTI image. It looks similar to 2D Gaussian distribution with mean equals to zero. In this case, the threshold processing is given by a certain circle in the complex plane with the center at $(0, 0)$.

The disadvantage of the method is that, in essence, the energy difference between the two images is used to determine the motion. The phase is not an informative random process. However, the simplicity of arranging threshold processing makes DPCA convenient to use.

Figure 3 represents a group of images that appear in DPCA processing.

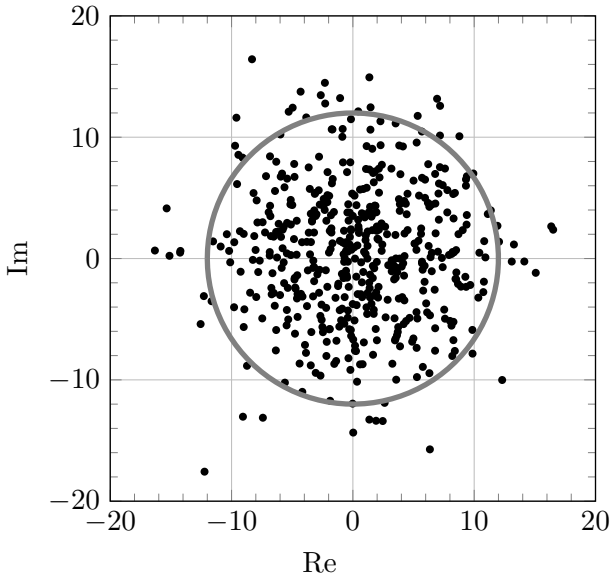

Figure 2. DPCA point distribution in GMTI image.

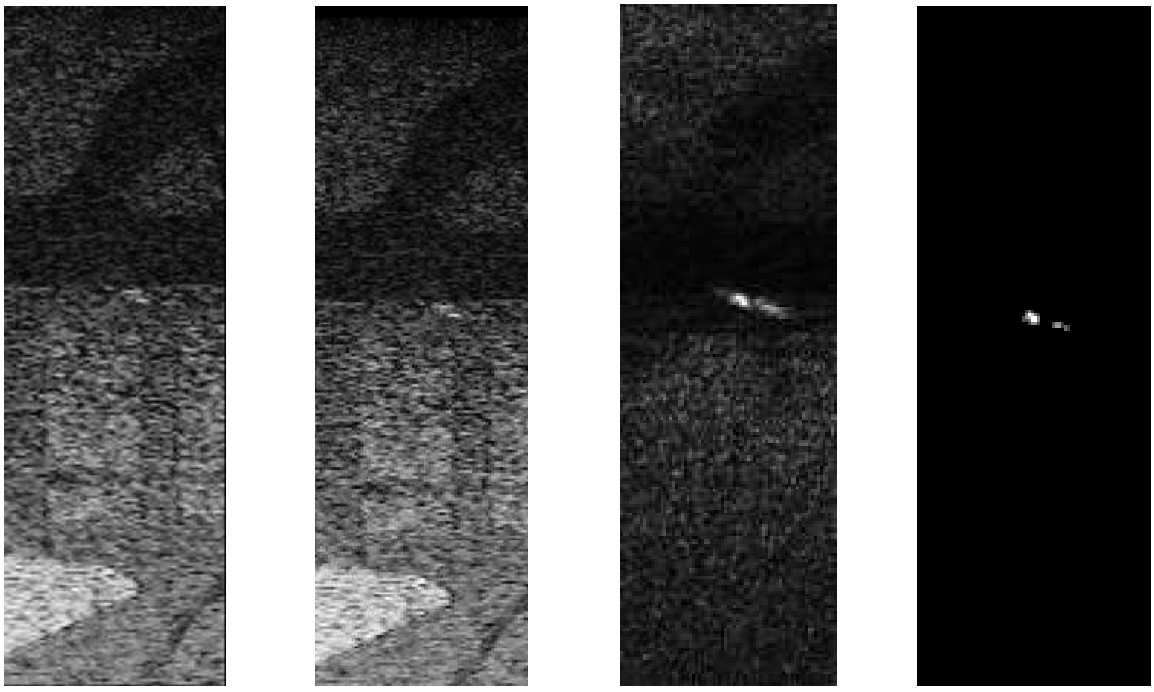

Figure 3. Radar images at different stages of GMTI: a) first radar image; b) second radar image; c) DPCA GMTI image; d) result of detection.

Figures 3(a) and 3(b) presents fragments of two common SAR images, that taken with small time delay. Along the road from left to right car moves with speed 100 km/h. A human eye can find some difference in the image, but if we use full SAR images it will be hardly possible. Figure 3(c) created by subtraction image 3(b) from 3(a), moving vehicle become the most bright object on the scene. Figure 3(d) represents the result of threshold detection. The object was deconstructed into two parts, but mostly result is pretty consistent.

4. Along-track interferometry algorithm

The basic idea of along-track interferometry algorithm is similar to DPCA algorithm. Two complex SAR images, taken under identical geometries separated by a short time interval, with the interferometric phase called "The ATI-SAR algorithm". Between phase centers of two antennas located along the track with separation B_x SAR data are collected in an ideal unsquinted (zero-Doppler) stripmap mode.

The form of the probability density of this points is described in equation (2).

$$f_c(\eta, \psi) = \frac{2n^{n+1}\eta^n}{\pi\Gamma(n)\cdot(1-|\rho|^2)} \cdot \exp\left(\frac{2n\eta\,|\rho|\cos(\psi-\theta)}{1-|\rho|^2}\right) \cdot K_{n-1}\left(\frac{2n\eta}{1-|\rho|^2}\right) \tag{2}$$

where n — number of views; $|\rho|$ — correlation coefficient; $\Gamma()$ — Gamma function; $K_n()$ — modified Bessel function n-th kind; θ — element that appears heterogeneous areas such as urban areas because of multi scattering effects in certain. In our work we assume that $\theta = 0$.

Equation 2 was derived in [9].

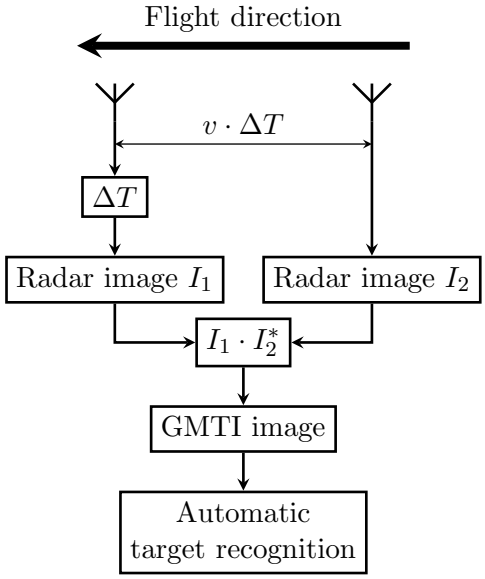

Figure 4. Image processing scheme using the ATI algorithm.

It is the more complicated way to separate points from moving targets from the background by using threshold processing, because of the form of distribution which presented in figure 5.

Interferometry of two images allows seeing differences in phase, which is more reliable with objects which have fast oscillating radar cross-section. Gray line in figure 4 represents an equipotential line of two-dimensional function presented in equation (2).

Figure 6 represents a group of images that appear in ATI processing.

Figures 6(a) and 6(b) is similar to 3(a) and 3(b) due to same experiment setup. Figure 6(c) represent result of $|I_1 \cdot I_2^*|$ operation. Similar figure 6(d) represent result of $\arg(I_1 \cdot I_2^*)$ operation. Figure 6(e) represents the result of threshold processing.

The resulting image is not so good as at figure 3(d), there is exist a false target below the main one. We think that is probably the fault of our implementation threshold selection. This is indirectly supported by the fact that a false target has a low amplitude and a large phase change. That does correspond to the clutter points with corrupted phase. That influence could be reduced for example by throwing away points with low magnitude. This issue was not considered in this work.

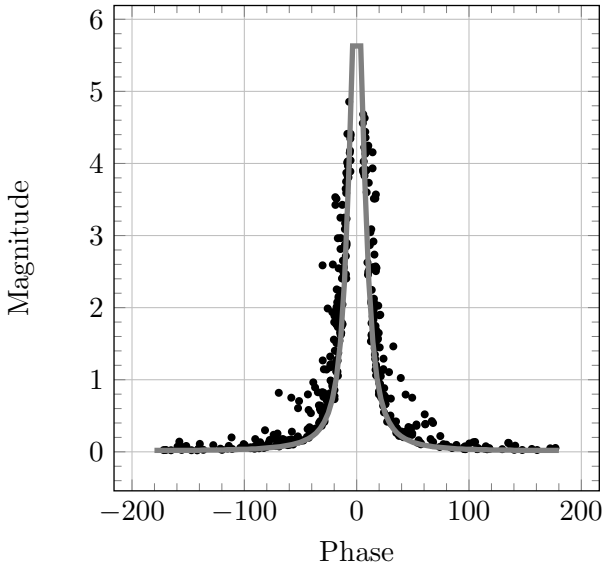

Figure 5. ATI point distribution in GMTI image (points of stationary targets are not included).

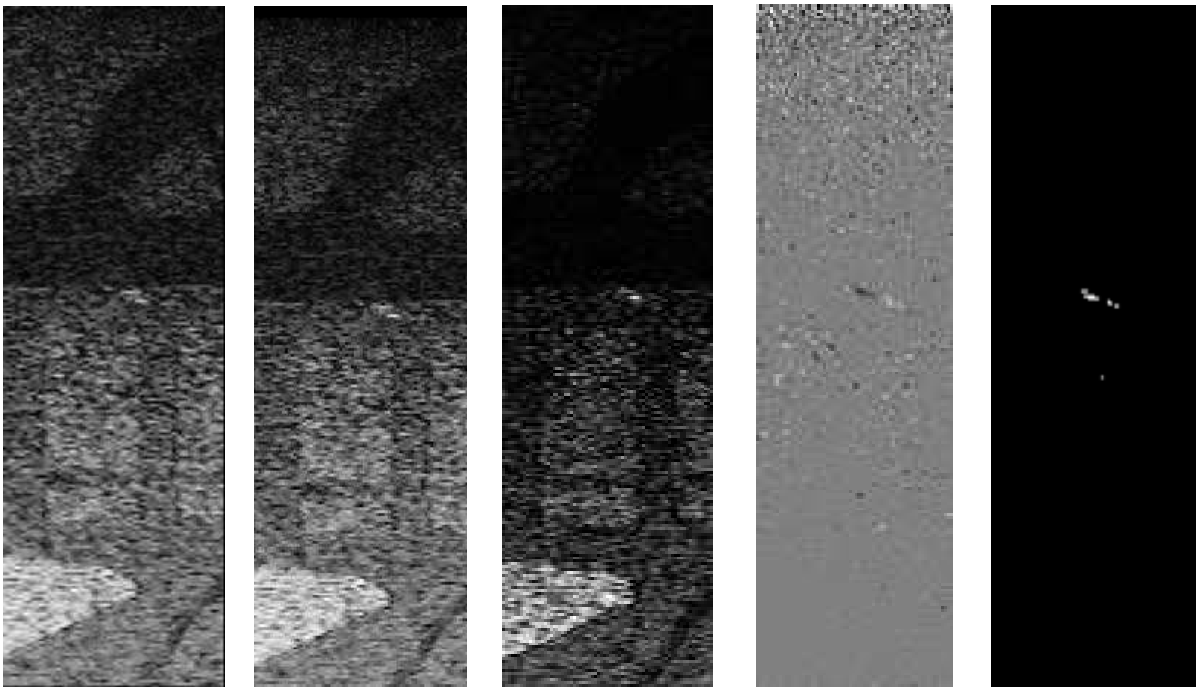

Figure 6. Radar images at different stages of ATI GMTI: a) first radar image; b) second radar image; c) magnitude after interferometry; d) phase after interferometry; e) result of detection.

5. Conclusions

In this paper, we presented complete image results of modeling GMTI processing algorithms for SAR. Algorithms show a pretty similar result. Figures 3(d) and 6(e) represent the results of processing GMTI with DPCA and ATI algorithms. Target on both images has divided into several parts. In figure 6(e) it is possible to see a small false target, but as we think ATI

algorithm has a potential in threshold processing due to utilizing not only magnitude plane, but the phase-magnitude plane. The use of a mathematical model with a lack of experimental data makes it possible to investigate various kinds of algorithms without limiting ourselves to the range of available wavelengths, the types of polarization, and the quality of the antenna system. In the future, it is possible to develop algorithms for multichannel GMTI SAR in that way.

6. **Acknowledgments**

The work is executed at financial support of the Ministry of Education and Science of the Russian Federation, project No. 2.2226.2017/Project Part and project No. 2.9140.2017/Basic Part.

The work is performed under financial support of Russian Found of Basic Research, research project No. 15-07-99514.

7. **References**

[1] Borzov, A.B. Mathematical Modeling and Simulation of the Input Signals of Short-Range Radar Systems / A.B. Borzov, V.B. Suchkov, B.I. Shakhtarin, Yu.A. Sidorkina // Journal of Communications Technology and Electronics. — 2014. - Vol. 59(12). - P. 1356–1368.

[2] Suchkov, V.B. Object-oriented method of determination of complex coefficients of reflection of elements of polygonal model of targets / V.B. Suchkov // Systems and means of communication, television, and broadcasting, 2013. [in Russian].

[3] Borzov, A.B. Digital modeling of the input signals of near-radar systems from complex radar scenes / A.B. Borzov, V.B. Suchkov, A.V. Sokolov // Journal Of Radio Electronics. — 2004. Vol. 4. [in Russian].

[4] Gordon, W.B. Far-Field Approximations to the Kirchhoff-Helmholtz Representations of Scattered Fields / W.B. Gordon // IEEE Transactions on antennas and propagation, 1975. - P. 590-592.

[5] Ufimtsev, P.Ya. Theory of Edge Diffraction of Electromagnetics / P.Ya. Ufimtsev // Tech Science Press Encino, California, 2003.

[6] King, C. A Survey of Terrain Radar Backscatter Coefficient Measure Program: CRES Technical Report 243–2 / C. King, R.K. Moore // TheUniversity of Kanzas, Center for Research Inc., 1973.

[7] Skolnik, M. Radar Handbook / M. Skolnik. — New York: McGraw Hill, 2008.

[8] Katz, I. Polarization and Depression-Angle Dependence of Radar Terrain Return / I. Katz, L.V. Spetner // Journal of Research of the National Bureau of Standards. — D. Radio Propagation. — 1960. — Vol. 64D — P. 483–486.

[9] Gao, G. Moving Target Detection Based on the Spreading Characteristics of SAR Interferograms in the Magnitude-Phase Plane / G. Gao, G. Shi, L. Yang, S. Zhou // Remote Sensing. — 2015. - Vol. 7. - P. 1836-1854.